

Porous palladium materials prepared by spark plasma sintering with addition of nano-pore-forming agent and surface treatment

WEI FENG^{a, b}, XIAODONG ZHU^{*a}, LIXIA PENG^c, XU ZHOU^a, JIAN LUO^a

^aDepartment of Material formation & control engineering, Chengdu University, Chengdu-610106, P.R. China

^bDepartment of Materials Science & Engineering, Sichuan University, Chengdu-610065, P. R. China

^cNational Key Laboratory for Surface Physics and Chemistry, Mianyang-621907, P. R. China

After the nano-palladium black particles as pore-forming agent were mixed with the spongy palladium powder, the porous palladium materials were prepared by using the spark plasma sintering and its surface was treated by using the redox. The results showed that, the nano-palladium black materials would produce significant shrinkage after being heated at 500°C–550°C and possess good pore-forming effect. After this pore-forming agent was mixed with the spongy palladium powder and sintered at 550°C, the porous palladium materials whose structural stability and mechanical properties were good, the pore size distribution and pore size could be adjusted effectively, the porosity was high (> 89%) could be prepared. Through analysis of surface composition, we could find that, the cleanliness of the materials was high since the addition of the pore-forming agent did not cause any pollution of materials. After surface treatment, the content of carbon impurity on the surface of the porous palladium materials could also be reduced to some extent so that surface roughness and surface area could be increased further.

(Received October 4, 2014; accepted June 24, 2015)

Keywords: Spark plasma sintering, Porous palladium, Nano-pore-forming agent, Surface treatment

1. Introduction

The palladium and its compound possess significant hydrogen isotope replacement performance [1-2], at present, have been extensively studied in the field of hydrogen energy [3-5]. As the equivalent materials of the palladium powder bed, the porous palladium bulk materials prepared by using the powder metallurgy technology possess higher structural stability and impact resistance, has been gradually applied in the hydrogen isotope displacement experiment [6]. However, there are some problem for the porous palladium materials prepared by using the powder metallurgy technology in the project application: Firstly, because the sintering temperature used by traditional power metallurgy technology is higher (700 °C–800 °C) [7], the size of the porous palladium particles is increased as well as their porosity and surface area are reduced so that its hydrogen isotope displacement rate is difficult to be improved. Secondly, because the spongy palladium powder and the porous palladium bulk possess stronger absorbability, their surfaces are easy to be affected by C impurity [8,9] so as to further cause their hydrogen isotope replacement efficiency was low [10, 11]. Finally, the inside of porous palladium sintered directly by using the spongy palladium powder is mostly composed of the aggregated pores having small pore size of the same

radius, which is adverse to increase the hydrogen absorption rate of the porous palladium materials [12, 13], however, in order that porous palladium materials bulk can be quickly covered with the hydrogen isotope molecules to make full use of specific surface area of the materials and be absorbed quickly by the scattered pores, during preparation of the porous palladium materials, it often has to add the specific pore-forming agent to adjust its pore structure. However, because the palladium powder and the porous palladium bulk possessed stronger absorbability [8], any pore-forming agent is inevitable to pollute the materials, which is extremely unfavorable to the porous palladium materials requiring very high cleanliness. Therefore, it need seek a suitable pore-forming method: both good porosity adjusting effect and no any pollution of materials, which will have broad application space for preparation the high-performance porous palladium materials and other high-performance porous metal materials.

The nano-palladium black has the same chemical composition as that of the spongy palladium powder, but almost doubled loose density of the spongy palladium powder, and apparent quantum [14, 15] size effect, and its melting point and sintering temperature are much lower than those of the spongy palladium powder. However, the nano-palladium black will be shrank and deformed during

sintering the porous palladium by directly using the nano-palladium black, which is difficult to meet the use requirements [6, 7]. Therefore, during preparation of the porous palladium, if it is feasible to exploit the favorable conditions and avoid unfavorable ones so as to both improve the pore structure of bulk materials by making full use of thermal stability of the spongy palladium and heat shrinkage of the nano-palladium black and avoid shrinkage, deformation, difficult pore adjustment and others, it will completely get rid of the pollution effect of the pore-forming agent and provide preparation of similar porous metal materials with a new pore-forming method for reference.

Therefore, in order to solve the above problems encountered in the project application process and perfect the preparation process of the porous palladium, main work of this paper was: (1) With the palladium black powder as the pore-forming agent, used the spark plasma pulse sintering (SPS) to prepare the porous palladium at lower temperature (500 °C —600 °C) so that it possessed high structural stability and obtained high porosity and pore structure. (2) Used the redox to treat the surface of the porous palladium so as to reduce the content of carbon impurity on the surface and improve the surface state of the porous palladium.

2. Experiments

2.1 Preparation of raw materials and SPS sintering process

The purity of the spongy palladium powder used in the experiment is 99.98%, with $1.414\text{g}\cdot\text{cm}^{-3}$ loose density, $3\mu\text{m}$ diameter. The nano-palladium black formed by agglomerating less than 10nm diameter palladium powder as raw materials is a kind of about $600\mu\text{m}$ diameter black particles, with 99.95% purity and $0.78\text{g}\cdot\text{cm}^{-3}$ loose density. The appearances of two kinds of raw materials powder refer to Fig. 1. The spongy palladium and the nano-palladium black are mixed with a mass ratio of 4:1 for later use [16]. In order to avoid breaking up the nano-palladium black particles, mechanical mixing time shall not be too long, about 2~3 min.

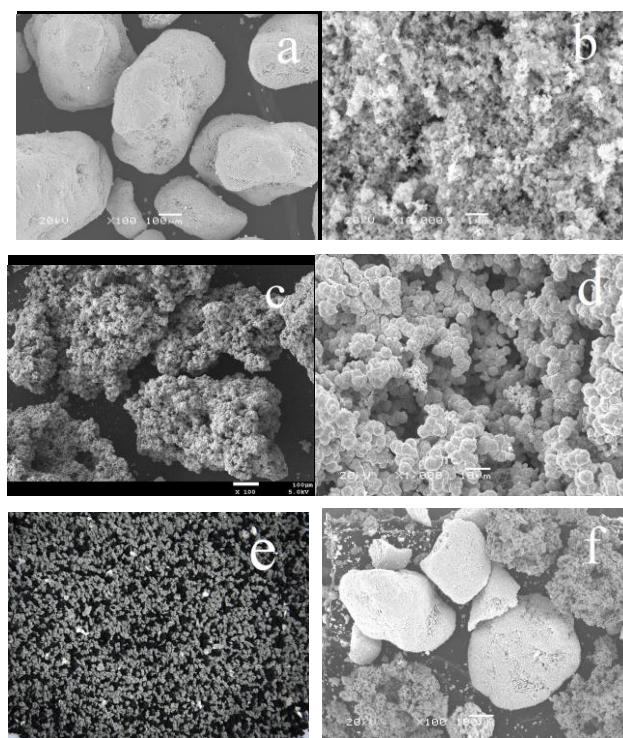


Fig. 1. Images of palladium powders. (a, b) nano-palladium black powders; c, d) spongy Pd powders; (e, f) mixture of palladium black and spongy Pd powders.

The sintering equipment used in the experiment is Dr Sinter SPS-1050 spark plasma sintering system (SPS). Unlike conventional SPS sintering method, in order to guarantee the porosity of the porous palladium materials and avoid compacting the powder under the action of thermal pressure, the die cavity volume is controlled by adjusting the height of the limit piece during the experiment and the mass of the added spongy palladium powder is determined according to the die cavity volume and the density of the spongy palladium powder. The parameters of SPS sintering are: the vacuity of sintering plant $3\times 10^{-2}\text{Pa}$, the sintering temperature 500 °C -600 °C, the sintering temperature rise rate $70\text{ }^\circ\text{C/s}$, the holding time after reaching the sintering temperature 3min, the die diagram and sintering diagram refer to Fig. 2.

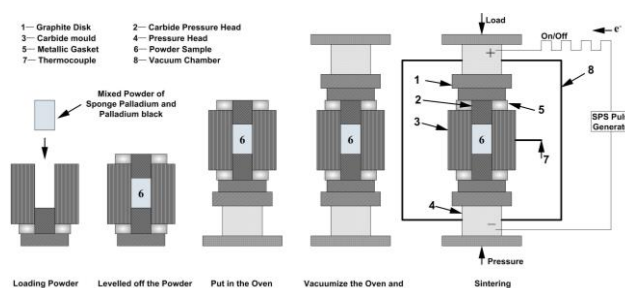


Fig. 2. Schematic representation of spark plasma sintering system and tungsten carbide mould.

2.2 Surface treatment of porous palladium

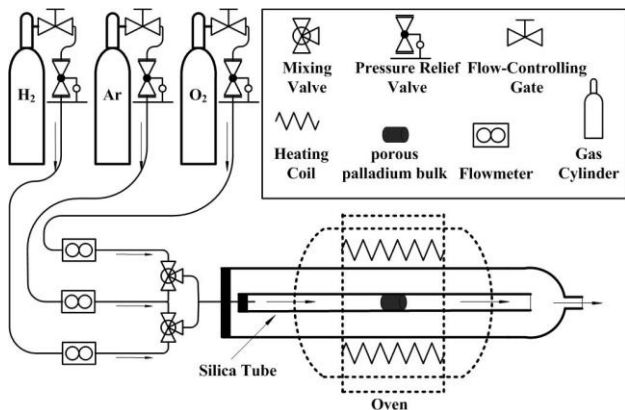


Fig. 3. Schematic of the apparatus used for the oxidation and deoxidation reactions.

The redox experiment of the porous palladium bulk material is carried out in the quartz tube furnace into which normal pressure air flow is input and the diagram of the experimental installation refers to Fig. 3. Firstly, put the porous palladium bulk materials into 16.00mm quartz tube ($\Phi=16.00\text{mm}$), then, aerate the argon gas (purity=99.999%, flow rate=15~20mL/s) to exhaust the air in the quartz tube and the porous palladium bulk. After adjusting the temperature of the quartz tube furnace to the reaction temperature, aerate the oxygen gas into the quartz tube (purity=99.999%, flow rate=15~20mL/s) and cut off the argon gas at the same time. After one hour reaction, aerate the argon gas again and gradually cut off the oxygen gas to take out of the bulk material after the temperature was reduced to the room temperature to finish the oxidation experiment of the porous palladium bulk material, inspect and analyze the results in the oxidation experiment. The reduction experiment of the porous palladium bulk material is the continuation of the oxidation experiment and the reduction temperature of all samples is the room temperature (23 °C). After the oxidation experiment, continue to aerate the argon gas and cool down the quartz tube along with the furnace to the room temperature. At room temperature, aerate the hydrogen gas into the quartz tube (purity=99.999%, flow rate=15~20mL/s), at the same time, cut off the argon gas. After one hour reaction, aerate the argon gas again and cut off the hydrogen gas to take the porous palladium out of the quartz tube bulk after the hydrogen gas is removed completely to finish the reduction experiment of the porous palladium bulk material, compare and analyze the results in the oxidation experiment. In the experiment, JSM-5600LV scanning electron microscope (SEM) is used, under 20kV, to observe the microscopic appearance on the fracture of the porous palladium bulk and ESCALAB Model 250 photoelectron spectroscopy is used to measure the chemical composition of the palladium materials and the fracture surface of the porous palladium bulk.

3 Results and analysis

3.1 Morphology evolution of nano-palladium black after heat treatment

For the purpose of adding the nano-palladium black as the pore-forming agent, on the one hand, adjust the pore size and pore size distribution of the porous palladium material by using its occupation function, on the other hand, optimize its porosity by using the heat shrinkage of the nano-materials, and its principle refers to Fig. 4[16].

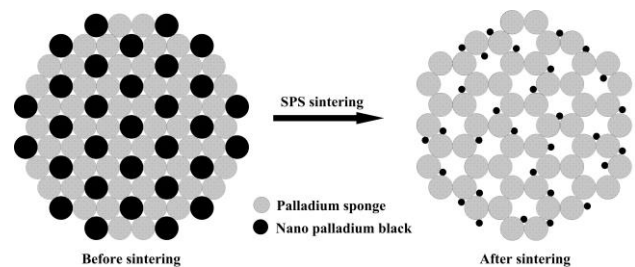


Fig. 4. Schematic diagram of the principles of nano-palladium black forming holes in palladium bulk.

By comparing the states before and after heating the nano-palladium black, we can find that, the nano-palladium black can keep the appearance similar to the original nano-palladium black after being heated at 500 °C, without apparent shrinkage change, as Fig. 1 (a) and Fig. 5 (a) shows. However, when the temperature is increased to 550°C, the nano-palladium black is shrunk obviously and its shrinkage is no longer increased further along with the temperature rise, as Fig. 5 (b, c) shows. By measuring the sizes of the nano-palladium black in Fig. 1 (a) and Fig. 5 (c), we can find that, when the temperature is increased to 550 °C, the diameter of the nano-palladium black is reduced to less than 1/2 diameter before being heated and its volume is reduced by more than 80% to meet the heat shrinkage target of the pore-forming agent in Fig. 4. It was interest to note that nano-palladium black with nanoporous microstructure can be obtained after sintering at 550 °C (as shown in Fig. 5d), which is beneficial to increase the surface area of the resultant porous palladium materials.

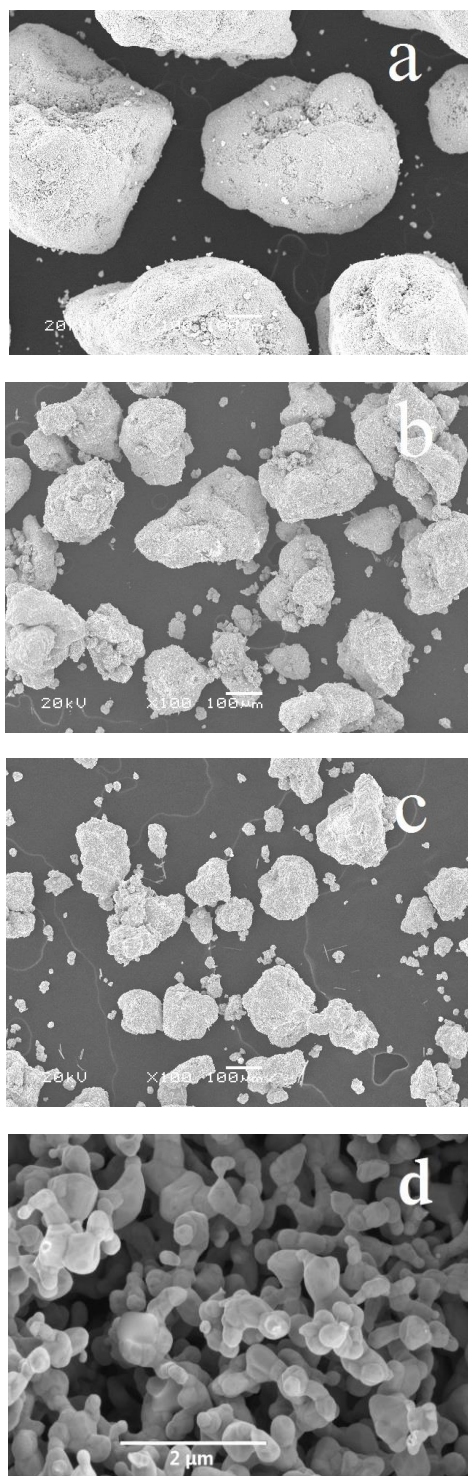


Fig. 5. Images (SEM) of the morphology changes of palladium black. (a) Sintering at 500 °C; (b) Sintering at 530 °C; (c) Sintering at 550 °C; (d) Enlargement image of Fig. 5(c).

3.2 Effect of the nano-palladium black pore-forming agent in preparation of the porous palladium materials

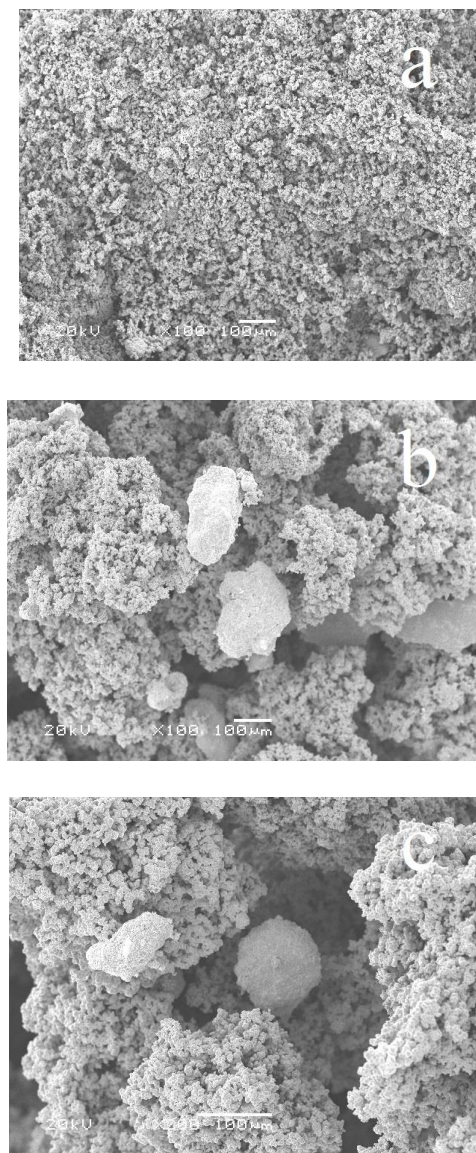


Fig. 6. Images (SEM) of internal morphology of the palladium bulks sintering at 550 °C. (a) Without any pore-forming agent; (b) Pore-forming by 20%(wt.%) palladium black; (c) The shrinkage of palladium black in the pore of palladium bulk; (d) The particles appearance inside the nano-palladium black powders.

Fig. 6 shows the microscopic appearance inside the porous palladium materials before and after adding 20% (wt. %) nano-pore-forming agent. It can be seen from Fig. 6 (a) that, the pore size in the porous palladium bulk materials by using SPS direct sintering and not adding the pore-forming agent is 10-20μm and the pores are almost completely composed of the pores in the spongy palladium powder as raw materials, without obviously

larger pores. Such small and dense pores are unfavorable for flow and replacement of the hydrogen isotope, as seen from table 1, the porosity of this porous palladium bulk is 87.94%. We can find from Fig. 6 (b) that, the pore-forming effect is obvious in the porous palladium bulk after shrinkage of the nano-pore-forming agent and larger pores with more than 500 μm diameter occur in the materials so that the pore size distribution of the materials is improved obviously. By analyzing Fig. 6 (c), we can find further that, there is obvious clearance between the nano-palladium black after shrinkage and the spongy palladium powder and the formed pore size is very close to the size of the pore-forming agent, which indicates the space left after shrinkage of the

nano-palladium black is not occupied by the spongy palladium powder. It can be seen from Table 1 that, the porosity of this porous palladium bulk is 89.82% and higher than that before adding the pore-forming agent so that the pore-forming effect of the palladium black is good. Fig. 6 (d) shows the particles appearance inside the nano-palladium black powders after being sintered at 550 $^{\circ}\text{C}$. It can be seen from it that, even if the nano-palladium black is shrank after being sintered at high temperature, its the structure will be still kept in the porous state that is composed of 200-300nm particles, therefore, such pore-forming agent can also achieve good effect of absorbing and exhausting the hydrogen gas in the project application.

Table 1. The structure parameters changes of the porous palladium bulk materials before and after adding the palladium black as the pore-forming agent.

Content of Pd Black (wt. %)	Quality of Pd Powder (g)	Sintering Temperature ($^{\circ}\text{C}$)	The Size of Pd Bulks		Quality of Pd Bulk (g)	Porosity of Pd Bulks (%)
			Diameter (cm)	Height (cm)		
0	5.35	23 $^{\circ}\text{C}$	1.55	2.00	5.35	88.28
0	5.35	550 $^{\circ}\text{C}$	1.54	1.93	5.24	87.94
10	4.86	550 $^{\circ}\text{C}$	1.54	1.97	4.82	89.13
20	4.60	550 $^{\circ}\text{C}$	1.54	1.95	4.47	89.82
30 (reject)	2.19	550 $^{\circ}\text{C}$	/	/	/	/

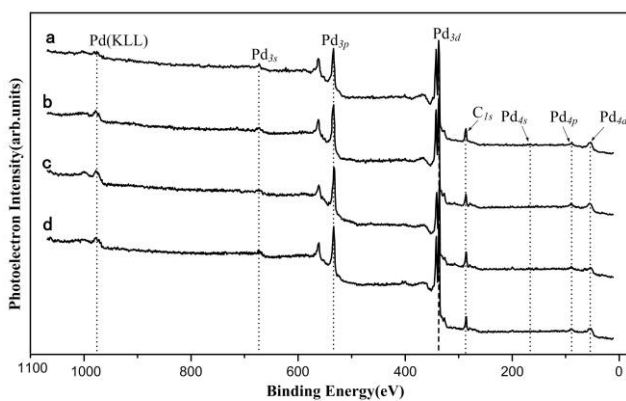


Fig. 7. The XPS patterns of the chemical composition on the surface of (a) spongy Pd powders; (b) palladium bulks without any pore-forming agent; (c) palladium bulks with 10%(wt.%) pore-forming agent; (d) palladium bulks with 20%(wt.%) pore-forming agent.

Fig. 7 shows the chemical composition on the surface of the porous palladium materials before and after adding nano-palladium black. It can be seen from figure that, there is not any other pollution element on the surface of the porous palladium materials except for C

impurity. Because C element is not the substance contained in the pore-forming agent and external contaminant induced from sintering, transportation or measurement, with respect to using the addition of the palladium black pore-forming agent to sinter the surface of the porous palladium materials, the addition of the palladium black pore-forming agent will not cause any pollution of the porous palladium materials.

3.3 Influence of the surface treatment on the surface state of the porous palladium materials

It can be seen from Fig. 7 that, whether the spongy palladium powder or the porous palladium bulk materials, except for C element, any other pollution element is not detected obviously, which indicates the contaminants on the surface of the porous palladium are mainly free C and its compound, and the relative content of C element is 34.3%—48.7%. Therefore, in order to improve the performance of the porous palladium bulk materials, it must try to remove the carbon pollutants on the surface of the palladium particles.

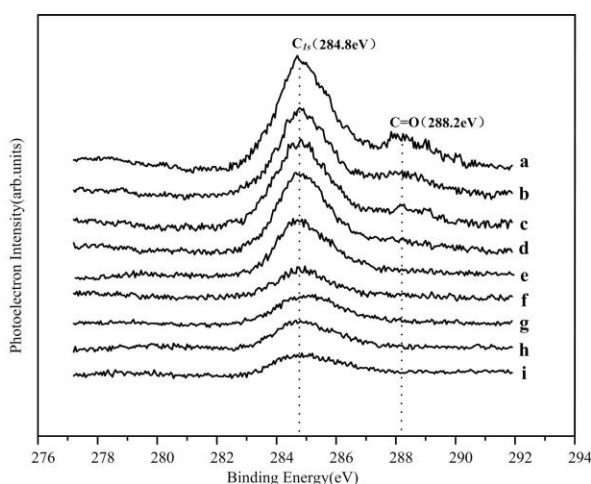


Fig. 8. XPS patterns of the variations in C spectra (XPS) on the surface of Pd Sponge powder and the porous palladium bulk sintering at 550 °C as a function of redox reaction. (a) Pd Spongy powder; (b) Oxidized at room temperature; (c) Oxidized at 200 °C; (d) Oxidized at 230 °C; (e) Oxidized at 240 °C; (f) Oxidized at 270 °C; (g) Oxidized at 350 °C; (h) Oxidized at 430 °C; (i) Oxidized at 500 °C.

We can find from Fig. 8 that, C_{1s} (284.8 eV) peak on the surface of the porous palladium bulk is gradually weakened in response to the oxidation temperature rise, after the oxidation temperature reaches 270 °C, C_{1s} peak intensity has been weakened obviously and the content of C element is reduced greatly in the oxidation. In Fig. 8 (a, b, c, d), four spectral lines have one satellite peak of hydrocarbon double-bond at 288.2 eV, however, after 270 °C oxidation, this satellite peak disappears, which indicates the organics on the surface of the porous palladium bulk materials are completely removed after the oxidation. It can be seen from Fig. 9 that, the relative content of C element on the surface of the porous palladium is reduced from 43.7% before 270 °C oxidation to 13.2% after 270 °C oxidation, however, after the oxidation temperature continues to be increased, the relative content of C element is kept about 11% and not changed significantly along with the temperature rise. This may be the result that the porous bulk materials re-absorb free carbon impurity during the transportation and XPS detection and the relative content of C element has been reduce greatly after the redox treatment.

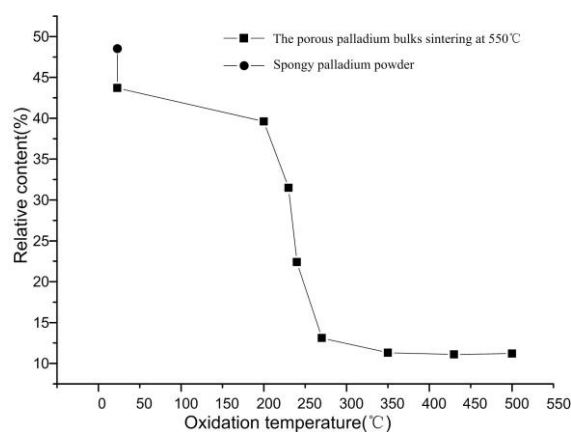


Fig. 9. Variation in the content of C on the surface of Pd bulk surfaces as a function of redox reaction.

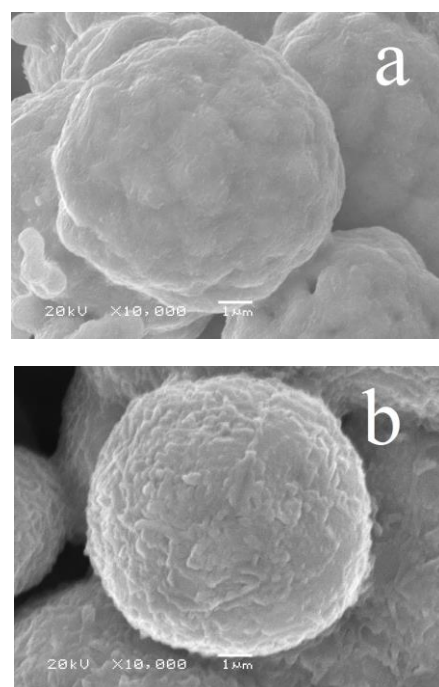


Fig. 10. Images (SEM) of internal particles morphology of the palladium bulks sintering at 550 °C. (a) Before redox reaction; (b) After redox reaction.

We can find from Fig. 10 (a) that, although the porous palladium bulk materials by 550 °C impulse sintering possess high porosity, uniform and loose structure of the palladium particles, good mechanical properties and other advantages, compared with the particles of the spongy palladium powder, the palladium particles inside such bulk materials are rounded slightly and their surface become also smoother. Fig. 10 (b) is the microscopic appearance of such porous palladium materials after 500 °C redox. It can be seen from figure that, after redox reaction, the size and structure of the palladium particles do not change obviously, however, during high-expansion observation of single palladium

particle, by comparing figure (b) with figure (a), we can find that obvious folds and more marks occur on the surface of the palladium particle so that the surface becomes rougher. On the one hand, the rough surface state can increase the surface area of the porous palladium materials, on the other hand, with respect to the catalysis, the rough surface can be used to further improve the surface catalytic capability and hydrogen isotope dissociative capability of the palladium particles, and such two capabilities are helpful to improve the hydrogen isotope displacement performance of the porous palladium materials.

4. Conclusion

1. After the nano-palladium black is heated at 500 °C -550 °C, its heat shrinkage is more than 80% and it possesses very strong heat shrinkage. The nano-palladium black after shrinkage has apparent pore-forming effect in the porous palladium bulk so that larger pores with more than 500µm diameter occur in the materials and the porosity is also increased by more than 1.8% by comparing with the porosity of the porous palladium materials without addition of the pore-forming agent to reach 89.82% to improve obviously the pore size distribution and porosity of the materials. The size of pore formed by shrinkage of the palladium black pore-forming agent is very close to the size of the pore-forming agent, which indicates the space left after shrinkage of the nano-palladium black is not collapsed, reduced or occupied by the spongy palladium powder and the pore-forming effect is good. After the nano-palladium black is shrunk through high-temperature sintering, its structure is still kept in the porous state and it still possesses good effect of absorbing and exhausting the hydrogen gas.

2. Except for C impurity, any other pollution element is not on the surface of the porous palladium materials prepared by using the nano-palladium black as the pore-forming agent and the addition of the palladium black pore-forming agent will not cause any pollution of the porous palladium materials. During redox treatment of the porous palladium bulk materials, after more than 270 °C oxidation and room temperature reduction, C element on the surface of the porous palladium materials can be reduced obviously. After 350 °C oxidation and room temperature reduction, C element on the surface of the materials is minimized. The redox treatment is an effective approach to solve C pollutant on the surface of the porous palladium materials.

3. After 500 °C oxidation and room temperature reduction of the porous palladium materials, obvious folds and marks occur on the surface of the palladium particles and the surface area of the porous palladium is increased so that the surface catalytic capability and hydrogen isotope dissociative capability can be improved.

Acknowledgement

Support by the Application and Foundation Research Projects of Sichuan Province under grant no.2014JY0119 and the Key Research Programs of Sichuan Province under grant no.2014GZ0004-5 are gratefully acknowledged.

References

- [1] William H. Fleming, Jamil A. Khan, Curtis A. Rhodes, *Hydrogen Energy* **26**, 711 (2001).
- [2] Lewis F. A. Hydrogen in palladium and palladium alloys, *Hydrogen Energy* **21**, 461 (1996).
- [3] E. Kikuchi, *Catalysis Today* **56**, 97 (2000).
- [4] Myung W. Lee, Ralph J. Wolf, John R. Ray, *Journal of Alloys and Compounds* **231**, 343 (1995).
- [5] R. Burch, F. J. Urbano, *Applied Catalysis A: General* **124**, 121(1995).
- [6] Meng Li, Ying Liu, Guangda Lu, *Rare Metal Materials and Engineering* **36**, 318 (2007).
- [7] Meng Li, Ying Liu, Guangda Lu, *International Journal of Hydrogen Energy* **18**, 5033 (2007).
- [8] S. Gredig, S. Tagliaferri, M. Maciejewski, *Studies in Surface Science and Catalysis* **96**, 285 (1995).
- [9] A. Ya. Tontegode, *Surface Science* **38**, 201 (1991).
- [10] Hou K, Hughes R, *Journal of Membrane Science* **206**, 119 (2002).
- [11] F. C. Gielens, R. J. J. Knibbeler, P. F. J. Duysinx, *Journal of Membrane Science* **279**, 176 (2006).
- [12] Li Meng, Yang Wenfeng, Liu Ying, *Rare Metal Materials and Engineering* **37**, 1766 (2008).
- [13] Feng Wei, Liu Ying, Lian Lixian, *Rare Metal Materials and Engineering* **42**, 1071(2013).
- [14] Y. X. Chen, B. L. He, H. F. Liu, *J Nanosci Nanotech* **21**, 187 (2005).
- [15] Peizhi Guo, Zhongbin Wei, Wanneng Ye, *Colloids and Surfaces A: Physicochemical and Engineering Aspects* **295**, 75 (2012).
- [16] Feng Wei, Liu Ying, Lian Lixian, Zhu XiaoDong, Kong Qingquan, *Rare Metal Materials and Engineering* **43**, 3159 (2014).

*Corresponding author: 50919808@qq.com